Evaluating the radiation dose around a hot cell after the bombardment of a Thorium target

Juliana Mendes

Department of Physics, Applied Physics and Astronomy, Rensselaer Polytechnic Institute, Troy, NY 12238

Kin Yip

Collider Accelerator Department, Brookhaven National Laboratory, Upton, NY 11973

Abstract

While Actinium-225 is promising for radiotherapeutic cancer treatments, there is a limited supply available for clinical trials. The proton spallation of Thorium is a method used to induce the production of Ac-225 as one of the daughter products in order to make this treatment more available. It is essential to evaluate and control the radiation dose during the process. The combination of Monte Carlo N-Particle eXtended (MCNPX) and CINDER90 was used as tools for simulating the bombardment of the Thorium target at 200 MeV for ten days. MCNPX is a transport code that tracks all the events and outcomes of each particle involved in the process. CINDER90 employed the resulting neutron flux data along with the production and destruction of isotopes to provide the decay gamma spectrum for requested time steps. The gamma spectrum is then used as a radiation source in MCNPX to evaluate the radiation dose at different locations near the modeled hot cell room in which the Thorium target was placed after the bombardment. Doses were measured in MCNPX immediately, three days and five days after the bombardment. This project has provided valuable information for the radiation safety of the workers around the hot cell room. It has also given me the opportunity to enhance my knowledge about nuclear physics and learn how to run Monte Carlo simulations in a supercomputer platform.

I. Introduction

The short half-lives of Actinium-225 (10 days) and its daughter product, Bismuth-213 (43 minutes), are ideal for cancer therapy treatments since its long enough for transportation to patients and short enough to avoid long-term storage in medical facilities. The benefits of these alpha-emitting isotopes are that unlike commonly used beta-emitting isotopes, they release highly energetic alpha particles in a short range, hence effectively eliminating the cancerous cells while leaving less healthy tissue harmed.[1] While these isotopes are very promising, they are scare throughout nature. Oak Ridge National Laboratory (ORNL) provides enough Actinium-225 to treat about 50 patients per year, but it is estimated that nearly 30 times as much is needed to conduct clinical trials.[2] At Brookhaven National Laboratory (BNL) isotopes for medical applications like these can be produced at the Brookhaven Linac Isotope Producer (BLIP). Small puck-shaped targets can be bombarded with highly focused beams of energetic protons at BLIP.[2] This proton spallation method is used to produce more Acinitum-225 by inducing decay in Thorium.

Although this bombardment has already been done at BLIP for many years, a different hot cell room has been proposed to place the irradiated target in the future. The gamma radiation emitted by the isotopes in the target can be a hazard to those who are around the hot cell room, and thus it is important to evaluate the dose rates. MCNPX version 2.7.0 and CINDER'90 can be used as tools to simulate the bombardment and estimate the dose rates at different locations that receive gamma radiation. MCNPX is a transport code that was developed at Los Alamos National Laboratory. It serves a purpose to track all the events of the particles present and to provide the probability of particle interactions by the use of physics models and a cross section library.[3] CINDER is a transmutation code that constructs a sequence of nuclide interactions to

provide a gamma spectrum for different time steps by using the data from MCNPX. The CINDER'90 package includes three additional components that allow the proper execution of the simulation: the "activation script", the "tabcode" and the "gamma source script". The "activation script" gathers necessary information from the MCNPX output files to prepare the execution for CINDER. The post-processing code, "tabcode", then employs these files to obtain the gamma spectra of the isotopes and the isotope inventory. The "gamma source script" combines the gamma spectra and provides the new source information for a new MCNPX input file. Once the hot cell room is modeled in the new MCNPX file, the simulation is then run again to evaluate the dose rates at different points around the hot cell room.

II. Methods and Process Outline

The first step of the process is modeling the target that will be bombarded at BLIP. The MCNPX input file is divided into three sections: cell cards, surface cards and data cards. The surface cards provide the geometric information of the stacked layers while the material cards provide the elements present in each material. The shape of the target is a right circular cylinder. This information is combined in the cell cards to construct the complete target. The details of the stacked materials can be seen in Table 1 and the 2-D image of the modeled target can be seen in Figure 1.

MCNPX is then run to simulate the bombardment with 200 MeV protons for 10 days. The proton is placed in front of the first layer of the target and was aligned in the z-axis. All the events caused by the particle interactions are recorded in a MCNPX output file called "histp", which will later on be used to extract information for CINDER to obtain cell based isotope production and destruction rates. The simulation is run until 100 million events are recorded.

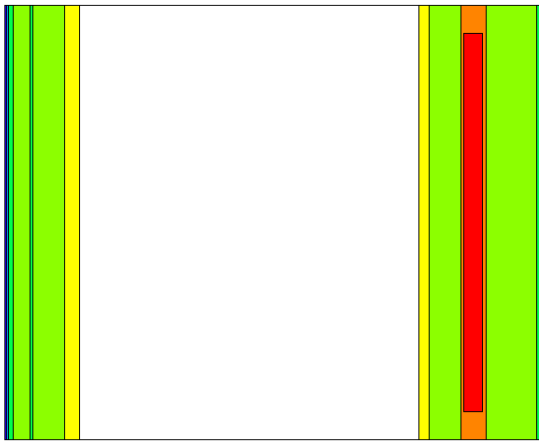

Fig. 1: 2-D image of the target modeled in MCNPX for bombardment.

Table 1: List of materials used for target

Layer Number	Material	Thickness (cm)	Density (cm/g^3)
1	Beryllium	0.0305	1.85
2	AlBeMet	0.0305	2.10
3	Stainless Steel	0.0787	8.0
4	Water	0.2682	1.0
5	Stainless Steel	0.0510	8.0
6	Water	0.5080	1.0
7	Copper	0.2410	8.96
8	Vacuum	5.4580	0
9	Copper	0.1580	8.96
10	Water	0.5080	1.0
11	Inconel	0.4070	8.43
12	Thorium	0.3050	11.7
13	Water	0.8100	1.0
14	Stainless Steel	0.0508	8.0

A shell script is used to execute the MCNPX file by providing the input and output file names. Two output files[a)], "histpa" and "histpb", are made to hold the information about the neutron fluxes averaged over the Inconel and thorium cells and the production and destruction rates of isotopes.

[a)] If there are too many events, there will be additional "histp" files (such as "histpa") produced.

A shell script was used to execute the more complex "activation script", which is written in Perl. All the necessary input and output files created from the CINDER package are placed in a separate directory for each cell in which the activation was performed. The first step for the activation process is reading the MCNPX output file to find the neutron fluxes and the material information for each cell. One of the files created in this directory contains the data of the neutron fluxes that provides the integral of all the fluxes and the fluxes separated into bins. All of these binned fluxes are multiplied by a normalization constant specified in the activation file which indicates the number of protons per second. To obtain this constant, the current of 200 μA is divided by the proton charge, resulting in 1.243E15 protons/s. The next step uses the code provided by the MCNPX package called "HTAPE3X". This code is executed by the activation script three times to evaluate the "histp" files. The code initially separates the information needed to generate the isotope production, gas production and isotope destruction data into files named "int8", "int14" and "int15", respectively. Each file is then evaluated by the same code to generate the mentioned data in the files "outt8", "outt14" and "outt15", respectively. The activation script then proceeds to read these output files in order to create a file containing the spallation products of each cell. The last file required for the execution of CINDER contains the information of the library path that contains a total of 3400 nuclides.[4]

After all these files are created in the directories made by the activation script, CINDER is finally ready to be executed. The main output of this process contains the initial and final nuclide information for each time step along with the total atom density activity for the Thorium and Inconel cells. The post-processing step utilizes "tabcode" to provide the final isotope inventory in different tables and the gamma spectra of the isotopes separated into 25 different energy bins for the requested time steps. After this process is done, a file indicating the cell

numbers in which an activation calculation was performed, the total volume, density and the directory name with the input and output files from the process is created.

The “gamma source script”, also written in Perl, utilizes that last file to locate the necessary files for its execution. The gamma spectrum acquired from the “spectra” file for each cell is combined to act as a photon source for the gamma radiation for the different time steps. The probability of the gamma radiation coming from either cell is determined by the cell weight, which is obtained by multiplying the weight per unit volume in the “spectra” file for each cell and its volume. The kinetic energy of the source is now a function of the energy bins and their probabilities. To obtain the probability of the energy of the photon coming from each bin, the gamma source script multiplies the cell weight by the gamma spectrum corresponding to each bin. Each source information for the different times will then replace the initial source information used for the target bombardment.

Since we want to know the dose rates outside of the hot cell room where the target gets placed in after the bombardment, it must also be modeled in MCNPX. The front view of the modeled hot cell room can be seen in Figure 2.

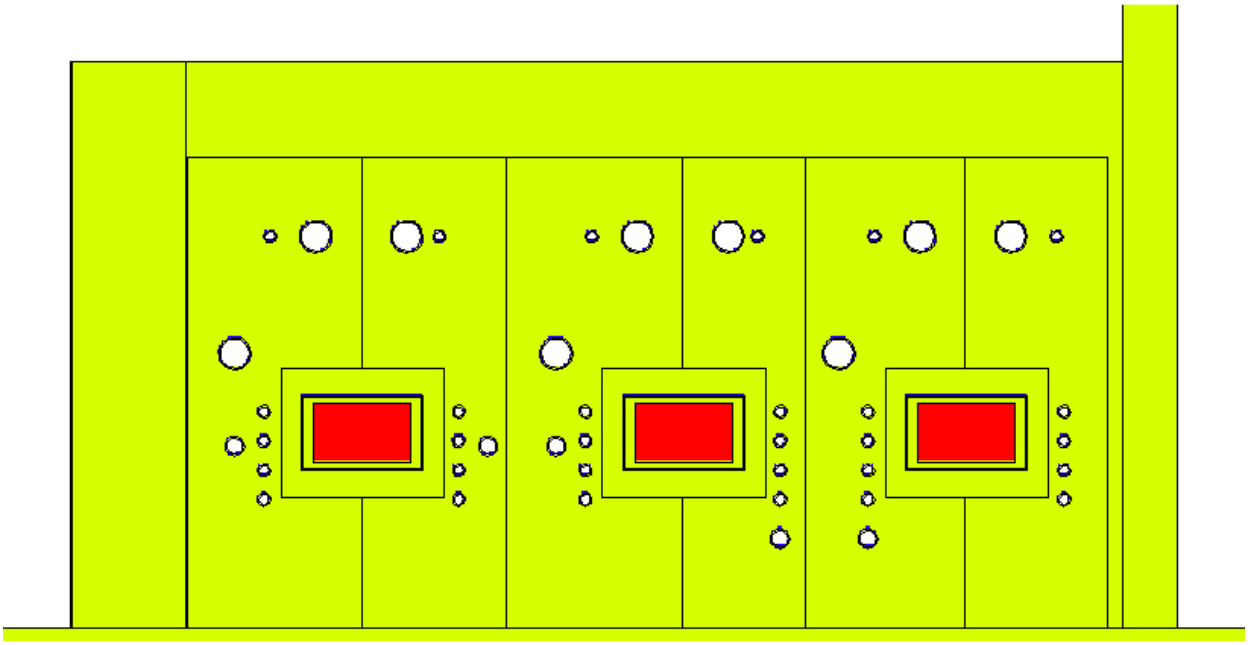

Fig. 2: Front view of the hot cell room beneath the outside steel liner modeled in MCNPX.

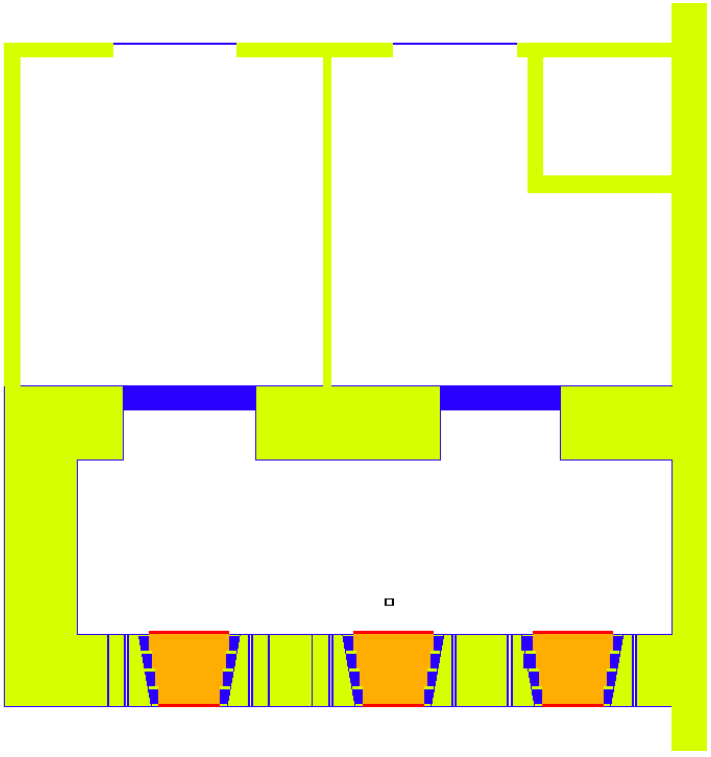

Fig. 3: Top view of the hot cell room modeled in MCNPX.

The target is placed 1.5′ from the middle lead glass window and 3′ above the floor. The hot cell room has a length of about 27′, height of 15′ and a width of about 10′. The room located behind the hot cell room was also modeled with the same length and height, but with a width of 17′. The top view of the hot cell room can be seen in Figure 3. The inside and outside of the hot cell room had a stainless steel liner 3/8″ thick. The two steel doors leading to the back area were each 1′ thick, while the other two steel doors leading to the outside of the modeled area were 8″. Three sides of the hot cell room were 3′ thick and made out of heavy concrete. The right side wall is 1.4′ thick. To account for the uncertainty of the material, two MCNPX files were made for the hot cell room, where one included heavy concrete for that wall and the other contained normal concrete. The material properties represented by the different cell colors can be seen in Table 2.

Table 2: Material properties of hot cell room

Cell Color	**Material**	**Density (g/cm^3)**
Green	Heavy Concrete	3.9
Blue	Stainless Steel	8.0
Orange	Lead Glass	6.2
Red	Non-browning Lime Glass	2.7
None	Normal Concrete	2.35

To evaluate the dose rates at different locations around the modeled room, detection tallies (F5) were implemented in the MCNPX input file to request 18 different point detectors. Each detector was either 10 cm or 1.5′ from the outside wall of the hot cell room. A dose function card was also included in the file to convert photon fluxes to the standard flux-to-dose conversion given by ICRP-21 1971.[5] A super computer platform named Cori at the National Energy Research Scientific Computer Center (NERSC) is utilized to run this simulation. Four sets of simulations are run with the irradiated target inside of the hot cell room: three with the

right side wall made out of heavy concrete for immediately, three days and five days after the bombardment and one immediately after the bombardment with normal concrete for the right side wall. Each simulation is run until 2 billion events were done.

III. Results and Discussion

The dose rates at the different time steps around the outside of the hot cell room in which all walls are made out of heavy concrete can be seen in Figures 4, 5 and 6. The dose rates immediately after the bombardment with normal concrete for the right side wall can be seen in Figure 7.

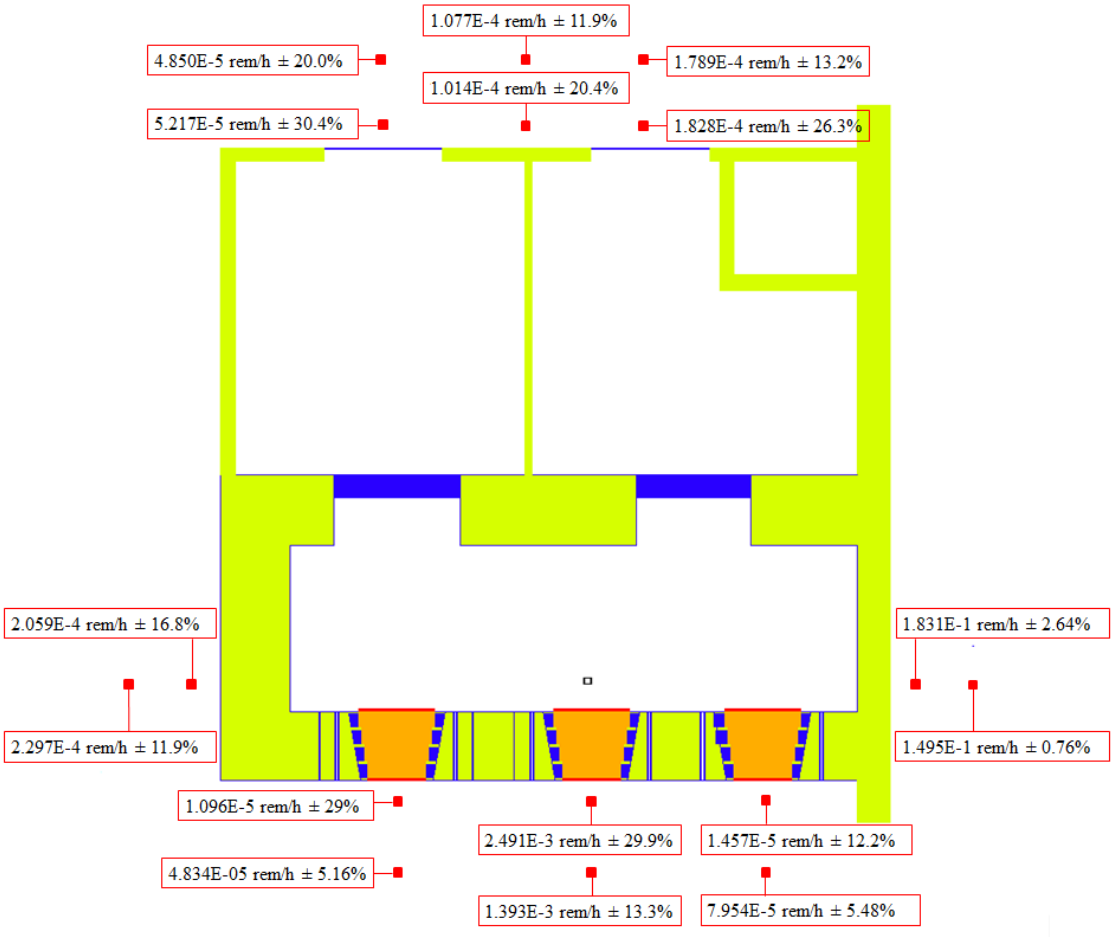

Fig. 4: Dose rates immediately after the bombardment.

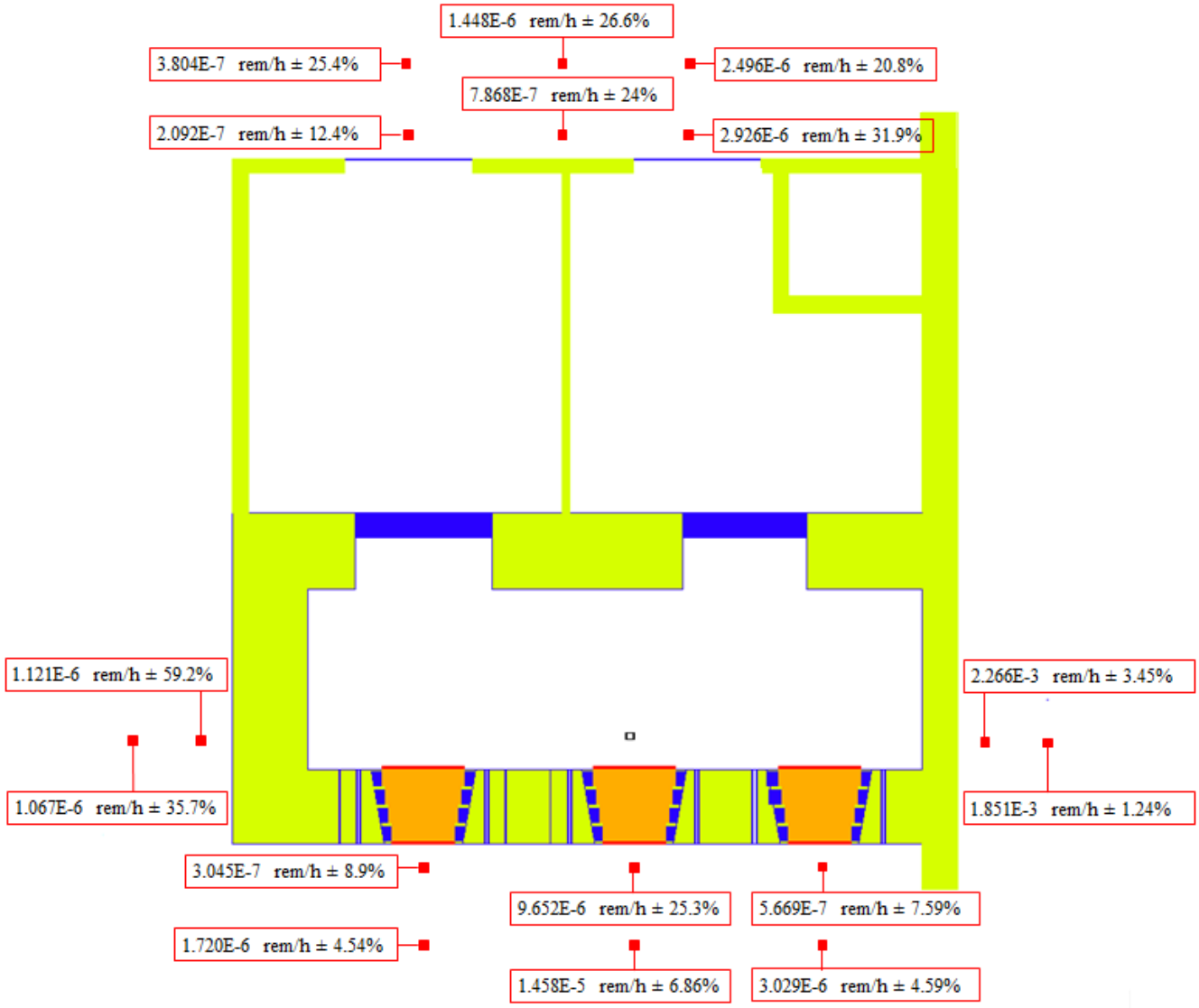

Fig. 5: Dose rates three days after the bombardment.

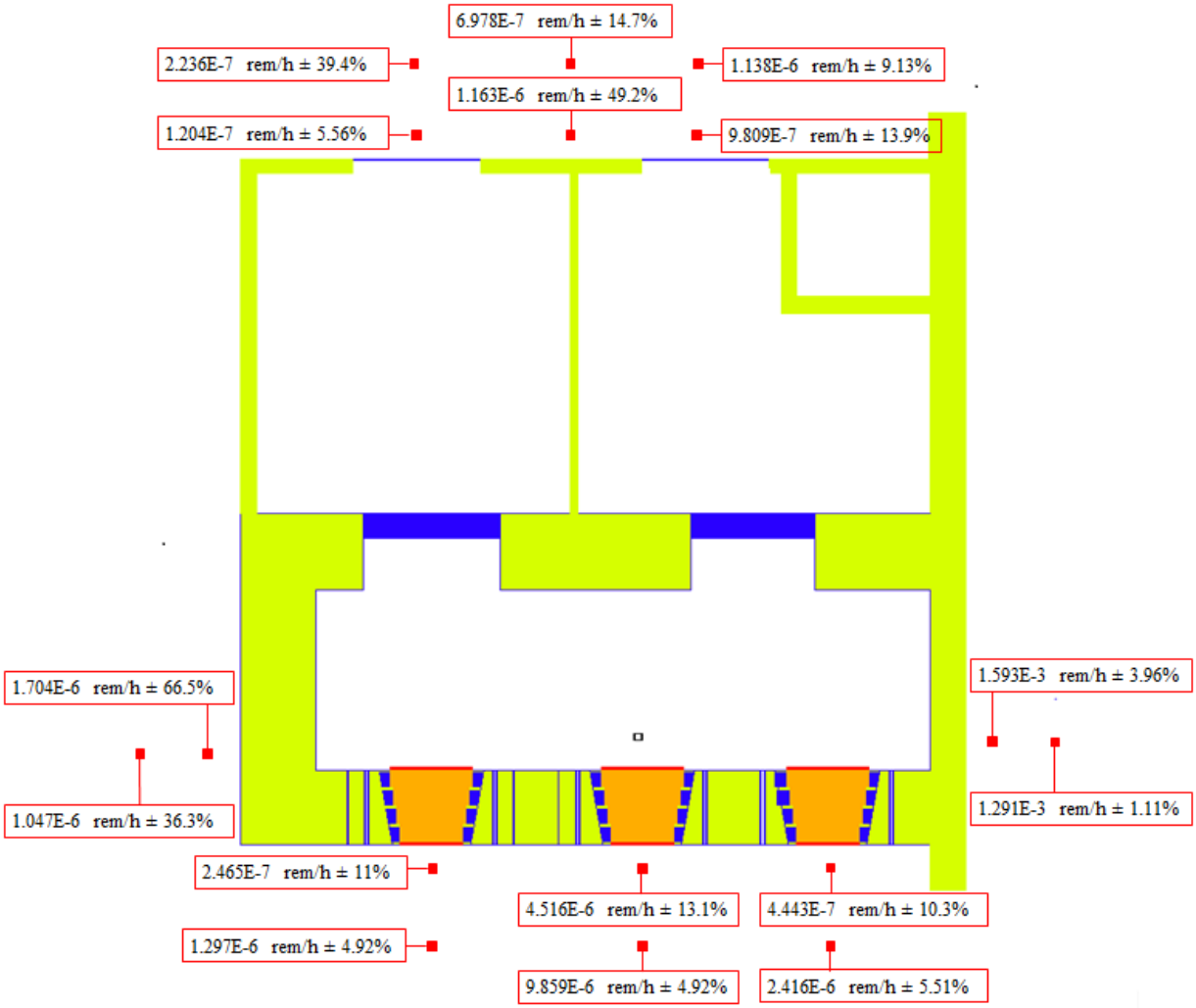

Fig. 6: Dose rates five days after the bombardment.

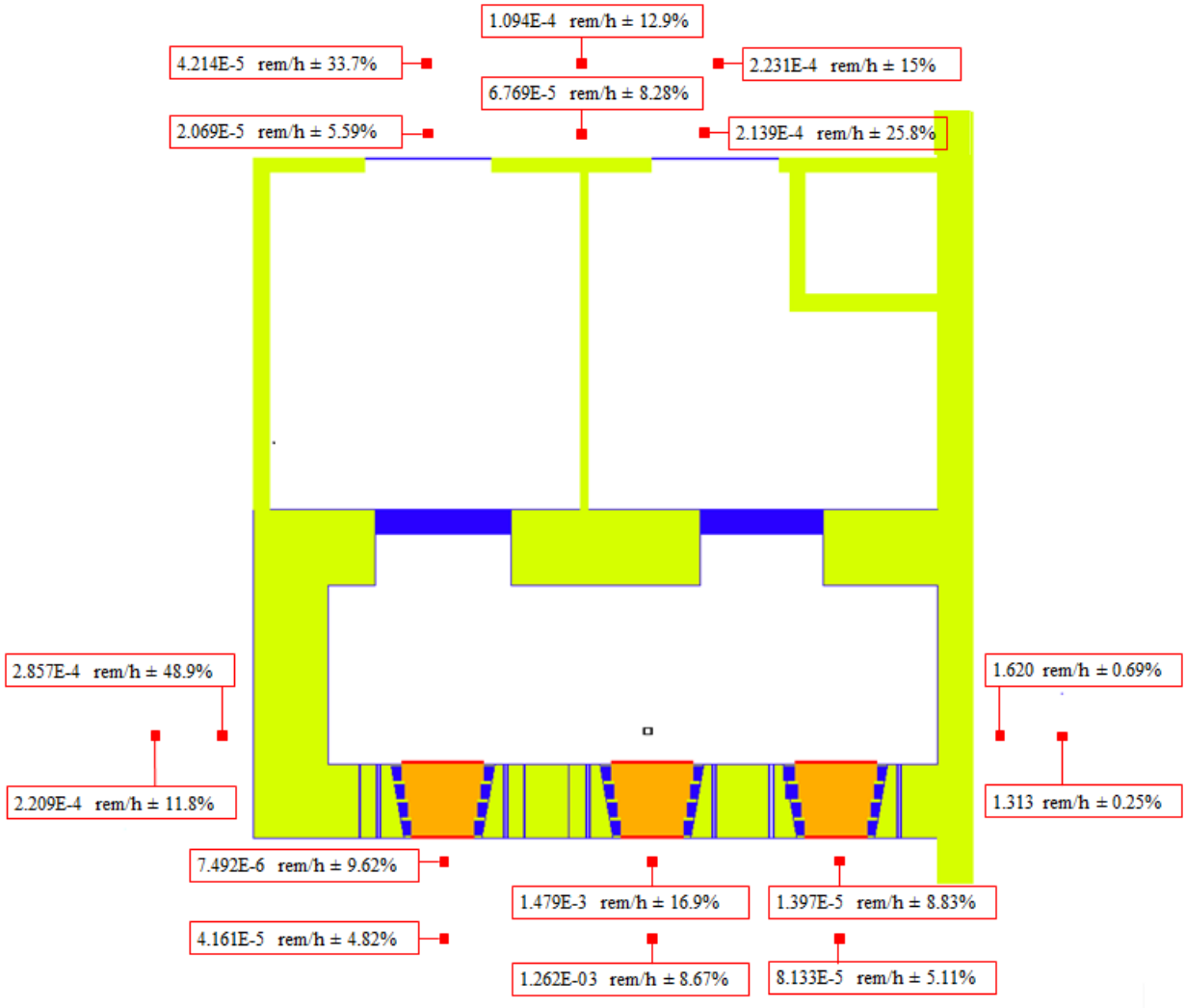

Fig. 7: Dose rates immediately after the bombardment with normal concrete for the right wall.

Although only 16 points can be seen in the figures above, the last two detectors are placed directly above the location of the target, at 10 cm (detector #17) and 1.5′ (detector #18), above the roof of the hot cell room. The estimated dose rates for these points at the different time steps can be seen in Table 3.

Table 3: Dose rates for the points located above the hot cell room

Time step of detection	Tally Number	Dose rates (rem/h)	Standard Deviation (%)
Immediately (Heavy Concrete)	17	1.629E-4	21.1
	18	2.124E-4	24.4
Immediately (Normal Concrete)	17	1.607E-4	23.9
	18	1.956E-4	17.1
Three Days	17	1.970E-6	62.9
	18	1.279E-6	34.0
Five days	17	8.776E-7	39.4
	18	9.048E-7	33.9

It can be seen that the highest dose rates are located near the right side wall in all time intervals. This was expected since this wall is thinner, allowing more gamma radiation to escape. When the simulation was run with normal concrete instead of heavy concrete for the right side wall, the estimated dose rate nearest to the wall increased from 0.183 rem/h ± 2.64% to 1.620 rem/h ± 0.69%, which is nearly 9 times higher. The other area with higher dose rates is directly in front of the middle window, where it was estimated to be 1.48E-3 rem/h ± 16.9% (closer point) and 1.26E-3 rem/h ± 8.67% (further point) immediately after the bombardment as seen in Figure 7. This was also predicted to be one of the areas of higher gamma radiation since it is the location closest to the irradiated target. There were many steel pipes inside the front wall, as seen in Figure 2, which could also have been a reason for the higher dose rates.

The reason why some of the standard deviations are relatively high is due to the fact that the corresponding dose rates or the Monte Carlo statistics are very low, causing small deviations to result in a high percent difference.

From the results mentioned above, it can be seen that one should avoid going close to especially the right side wall if the target is placed inside the hot cell room immediately after the

bombardment. Moreover, to reduce the radiation hazard, one can delay placing the target in the hot cell room after the bombardment; or one can build an additional shielding on the right side wall. The CINDER simulation provides a file containing an inventory of all isotopes resulted from the process. A sample of the acquired isotopes with the highest total activities can be seen in the Appendix in Table A1.

IV. Conclusion

The combination of MCNPX and CINDER was used as a tool to initially simulate the bombardment of a Thorium target and then to estimate the dose rates around the hot cell room where it is proposed to be placed after being irradiated in the future. The initial target was a stack of different elements, but then only the Thorium puck surrounded by Inconel was placed in the hot cell room for the simulation. The sets of simulations were run in a supercomputer platform until 2 billion events were done. The highest dose rate was estimated as 1.620 rem/h ± 0.69% at the location near the right side wall when made out of normal concrete. If the actual material is heavy concrete, then this dose rate was estimated to be 0.183 rem/h ± 2.64%. Workers around the hot cell room should especially avoid going near this area immediately after the bombardment. An inventory of the isotopes was also obtained throughout this process.

V. Acknowledgements

This project was supported in part by the U.S. Department of Energy, Office of Science, Office of Workforce Development for Teachers and Scientists (WDTS) under the Science Undergraduate Laboratory Internships Program (SULI).”

Appendix

Table A1: Sample of Isotope Inventory from CINDER

Isotope	Total Activity (Curies)
Th231	39.680
Th233	18.510
Ra222	13.160
Rn218	13.140
Th226	11.500
Bi211	9.738
Tl207	9.712
At215	9.109
Fr219	9.109
Ac223	9.096
Bi212	7.843
Ac224	7.640
Po214	7.277
Ac231	7.267
Rn220	7.258
Ra224	7.256
Po216	7.201
Ac226	7.086
Pb212	7.014
Fr218	6.347
I 132	6.166
At214	6.122
Xe135	6.054
I 133	5.900
At213	5.751
Fr217	5.750
La141	5.745
Ac229	5.696
Ac221	5.571
Ac222	5.457
Ba139	5.305
Cs138	5.118
Ac228	5.116
La142	4.822
Te129	4.792
Fr221	4.723
Ac225	**4.635**
Ce143	4.633
At217	4.597
Bi210	4.589
Bi213	4.582
Te127	4.556
Te132	4.363
Te131	4.281
Ba141	4.228
Pa233	4.182
I 135	4.108
Pr145	4.057
I 131	4.045
Cs139	3.948
Xe138	3.752
La143	3.751
Cs140	3.681
Xe137	3.678
Ba142	3.659
Pa229	3.561
Pr146	3.327
Ac230	3.303
La144	3.285
Te134	3.273
Ce145	3.148
Cs141	3.065
La140	3.013
Fr216	2.937
Te133	2.895
I 136	2.851
Tl208	2.819
Ac220	2.791
Ce146	2.696
Pb209	2.654
Pr147	2.651
Po213	2.559
Rn217	2.559
Ra221	2.557
Ba143	2.467
La145	2.403
Ba144	2.356
Th227	2.356
I 137	2.329
Xe140	2.313
Pm149	2.268
Ba140	2.259
Xe139	2.241
Cs142	2.219
At211	2.045
Po211	2.020
I 138	2.009
Pr148	1.991
Nd149	1.917
Pr143	1.914
Ce147	1.890
Te136	1.844
Fr215	1.781
Po212	1.771
Rn216	1.769

Te135	1.738
Th225	1.705
I 130	1.620
Pa228	1.576
I 128	1.556
Ac219	1.552
Pm151	1.539
La146	1.531
Xe141	1.529
Pr149	1.524
Cs143	1.490
Ce148	1.469
Nd147	1.462
Pa232	1.408
Ba145	1.406
Pa230	1.396
La147	1.357
Ce141	1.262
Rn219	1.255
Ra223	1.254
Cs144	1.168
Xe142	1.164
Ba146	1.130
Pr150	1.116
I 139	1.105
Nd151	1.104
Pm152	1.079
La135	1.063
Te138	1.029
Sm153	1.003
Ce149	0.962
I 140	0.950
Te137	0.929
Cs129	0.910
I 123	0.894
Nd152	0.875
La148	0.866
Pr144	0.851
Rn214	0.851

Pa227	0.846
Ra218	0.827
La136	0.809
Pm153	0.806
Cs136	0.801
Rn215	0.800
Pr151	0.798
Ra219	0.789
Cs132	0.781
Ce150	0.760
Cs145	0.759
Pr140	0.752
Cs130	0.728
Ce137	0.699
Ra227	0.695
Cs131	0.690
La134	0.661
Ba147	0.644
Pr142	0.644
At210	0.643
I 141	0.640
I 124	0.638
Po215	0.630
Pb211	0.629
Th224	0.617
Xe144	0.599
La149	0.595
Rn212	0.595
Sm155	0.585
Cs128	0.553
Pr152	0.546
Cs146	0.539
Te140	0.537
Fr214	0.527
Rn213	0.515
Pr139	0.515
Ba148	0.505
Nd153	0.494
Ra216	0.491

I 126	0.483
Ra217	0.479
I 142	0.477
Xe125	0.476
Eu157	0.465
Xe143	0.462
La133	0.452
Ce151	0.442
Sm156	0.440
Ac218	0.421
Ra225	0.413
Pm155	0.407
At209	0.394
La150	0.389
Nd154	0.380
Cs127	0.379
I 143	0.365
Cs147	0.364
Gd159	0.362
Ra229	0.352
Nd141	0.349
I 121	0.344
Pm150	0.335
Eu158	0.333
Rn211	0.332
Ce135	0.289
Te121	0.280
Ra215	0.278
Rn210	0.272
Xe145	0.270
Tb162	0.260
Ba131	0.259
Pm156	0.259
Eu159	0.255
Pa226	0.254
Te142	0.251
Ra214	0.244
La132	0.243
Te139	0.241

Te118	0.227
I 144	0.224
Cs126	0.223
Sm158	0.223
La151	0.222
Ra230	0.219
Nd140	0.219
Gd161	0.217
Pr138	0.217
Cs148	0.215
Eu156	0.215
Pr154	0.212
Tb161	0.210
Po210	0.205
Th228	0.204
Pr137	0.199
Ba150	0.197
Tb163	0.197
I 125	0.186
Pm157	0.186
Xe127	0.184
Eu160	0.184
Gd162	0.173
Ce134	0.172
Xe123	0.166
I 145	0.165
Dy165	0.165
Ho166	0.165
Ho167	0.164
Ba128	0.163
La131	0.161
Pm148	0.160
Nd156	0.157
I 120	0.151
Te141	0.150
Ba129	0.146
Po206	0.146
Cs149	0.145
La152	0.144
Tb164	0.144
Sm159	0.138

Eu161	0.135
Te117	0.132
Dy166	0.132
Ho168	0.131
Cs125	0.131
Pm142	0.131
Ce153	0.130
Po207	0.126
Pr155	0.122
Bi206	0.122
Ac232	0.120
Pm158	0.118
Ce154	0.114
Gd163	0.113
Ac217	0.113
Xe147	0.109
Tb165	0.108
Ce144	0.107
Eu162	0.101
Xe122	0.100
Pr136	0.100
Te144	0.098
Dy167	0.098
Tl209	0.097
Nd139	0.096
Tb166	0.095
Xe148	0.094
Fr212	0.093
I 119	0.089
Er171	0.088
Gd164	0.088
Te116	0.088
Ho169	0.088
Nd157	0.088
Ra213	0.085
Th223	0.083
Dy168	0.083
Tm172	0.082
La153	0.082
Pa225	0.082
Pm141	0.080

La130	0.079
I 146	0.078
Te143	0.077
Fr223	0.075
Ba127	0.075
Fr222	0.074
Pm159	0.074
Sm161	0.072
Nd138	0.072
Rn209	0.071
Tm173	0.069
Tb155	0.069
Ba152	0.068
Ce139	0.068
Nd158	0.068
Ba151	0.068
Er172	0.067
Pr156	0.065
Er169	0.065
At208	0.064
Er165	0.063
Tb167	0.062
Sm162	0.058
Tm174	0.058
Fr224	0.058
Eu163	0.058
Gd165	0.058
Cs150	0.058
Ho171	0.057
Ce132	0.057
Dy157	0.057
Ho170	0.055
Tb156	0.054
Gd166	0.054
Cs124	0.054
Ho164	0.053
Yb175	0.052
Ho162	0.052
Ba126	0.051
Pr135	0.051
Dy169	0.050

References

[1] Idaho National Laboratory. "Medical Actinium for Therapeutic Treatment (MATT)." < http://www4vip.inl.gov/factsheets/docs/matt.pdf>.

[2] Walsh, K. M. “Producing radioisotopes for medical imaging and disease treatment." Mar 2017. < https://www.bnl.gov/newsroom/news.php?a=212043>.

[3] Hughes, H. G. & James, M. R. Los Alamos National Laboratory. “MCNP6 Class”. Feb 2014. < http://permalink.lanl.gov/object/tr?what=info:lanl-repo/lareport/LA-UR-14-21281>.

[4] Trellue, H. R., Fensin, M. L., & Galloway, J. D. Los Alamos National Laboratory. “Production and Depletion Calculations Using MCNP” < https://mcnp.lanl.gov/ pdf_files/la-ur-12-25804.pdf>.

[5] Biswas, D. Westinghouse Safety Management Solutions LLC. “Rad-in-Tissue versus Rad-in-Air” < http://sti.srs.gov/fulltext/ms2002472/ms2002472.html>.